Drug Design, Development and Therapy

Dovepress

open access to scientific and medical research

Open Access Full Text Article

ORIGINAL RESEARCH

# Carbon Monoxide-Releasing Molecule-3 Enhances Osteogenic Differentiation of Rat Bone Marrow Mesenchymal Stem Cells via miR-195-5p/Wnt3a Pathway

Jingyuan Li[1], Qingbin Han[2], Hui Chen[3], Tingting Liu[1], Jiahui Song[1], Meng Hou[4], Lingling Wei[1], Hui Song[1]

[1]School and Hospital of Stomatology, Cheeloo College of Medicine, Shandong University & Shandong Key Laboratory of Oral Tissue Regeneration & Shandong Engineering Laboratory for Dental Materials and Oral Tissue Regeneration, Jinan, People's Republic of China; [2]Department of Oral and Maxillofacial Surgery, Shandong Linyi People's Hospital, Linyi, People's Republic of China; [3]Department of Endodontics, Jinan Stomatological Hospital, Jinan, People's Republic of China; [4]School of Stomatology, Jining Medical College, Jining, People's Republic of China

Correspondence: Hui Song, School and Hospital of Stomatology, Cheeloo College of Medicine, Shandong University & Shandong Key Laboratory of Oral Tissue Regeneration & Shandong Engineering Laboratory for Dental Materials and Oral Tissue Regeneration, Jinan, 250012, People's Republic of China, Tel +86-531-88382912, Fax +86-531-88382923, Email songhui@sdu.edu.cn

**Purpose:** Bone marrow-derived mesenchymal stem cells (BMSCs) are hopeful in promoting bone regeneration as their pluripotency in differentiation. Our previous study showed that carbon monoxide-releasing molecule-3 (CORM-3) increased the osteogenic differentiation of rat BMSCs in vitro. However, the mechanism remained unclear. MicroRNAs (miRNAs) play a very important role in modulating the osteogenic differentiation of BMSCs. Therefore, we researched the miRNAs involved in CORM-3-stimulated osteogenic differentiation.

**Methods:** The CORM-3-stimulated osteogenic differentiation of rat BMSCs was further studied in vivo. Based on the gene sequencing experiment, the rat BMSCs were transfected with miR-195-5p mimics and inhibitor, pcDNA3.1-Wnt3a and Wnt3a siRNA. The osteogenic differentiation of rat BMSCs was measured by quantitative real-time polymerase chain reaction, Western blot and alizarin red staining. Additionally, the targeting relationship between miR-195-5p and Wnt3a was confirmed by the dual-luciferase assay.

**Results:** MiR-195-5p was down-expressed during the CORM-3-stimulated osteogenic differentiation of rat BMSCs. CORM-3-stimulated osteogenic differentiation of rat BMSCs was inhibited with miR-195-5p overexpression, evidenced by significantly reduced mRNA and protein expressions of runt-related transcription factor 2 and osteopontin, and matrix mineralization demonstrated. On the contrary, the osteogenic differentiation was enhanced with inhibition of miR-195-5p. CORM-3-stimulated osteogenic differentiation of rat BMSCs was increased by overexpression of Wnt3a, while the opposite was observed in the Wnt3a-deficient cells. Moreover, the decreased osteogenic differentiation capacity by increased expression of miR-195-5p was rescued by Wnt3a overexpression, showing miR-195-5p directly targeted Wnt3a.

**Conclusion:** These results demonstrate that CORM-3 promoted osteogenic differentiation of rat BMSCs via miR-195-5p/Wnt3a, which bodes well for the application of CORM-3 in the treatment of periodontal disease and other bone-defect diseases.

**Keywords:** carbon monoxide-releasing molecule-3, microRNA-195-5p, Wnt3a, osteogenic differentiation, bone marrow mesenchymal stem cells

## Introduction

Repairing and reconstruction of bony defect remains a crucial clinical challenge. Bone marrow-derived mesenchymal stem cells (BMSCs) are pluripotent cells that can differentiate into many kinds of cells, such as bone, skeletal and cardiac muscle, adipose tissue, and neural cells.[1–3] Numerous studies have showed that BMSCs are potential in promoting bone regeneration and defect repair, as they are capable of differentiating into osteoblasts.[1,4]

Received: 23 March 2022
Accepted: 25 June 2022
Published: 2 July 2022

**Graphical Abstract**

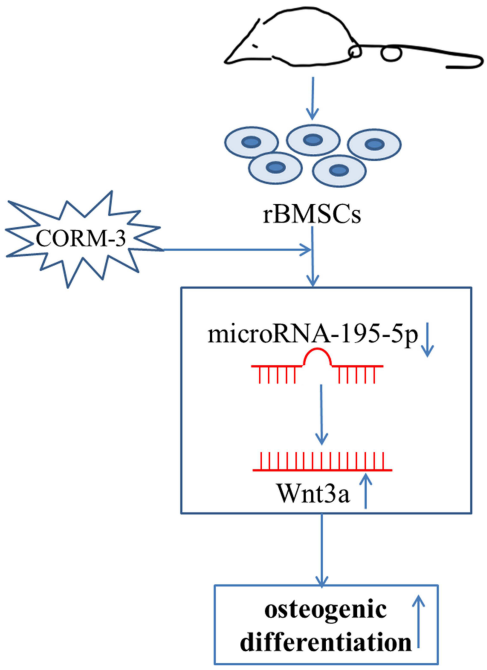


MicroRNAs (miRNAs) are non-coding RNAs, which are approximately 22 nucleotides in length. miRNAs play an important role in the post-transcriptional regulation of gene expression by interacting with the 3′ untranslated region (3′ UTR), which induces mRNA degradation or suppresses protein translation.[5–7] Lots of miRNAs have been defined as regulators of osteogenic differentiation and osteogenesis, either positively or negatively, through different signaling pathways.[8–10] miRNAs have a significant impact on regulating the osteogenic differentiation of BMSCs.[11,12] For example, miR-149-3p modulates the switch between adipogenic and osteogenic differentiation of BMSCs by targeting FTO.[13] Moreover, miR-488 negatively regulates the psoralen-stimulated osteogenic differentiation of BMSCs via targeting Runx2.[14]

Carbon monoxide-releasing molecules (CORMs) are transition metal carbonyl-based compounds, able to sustainedly release CO.[15] CORM-3 is a newly synthesized water-soluble form of metal carbonyl. 1 mole of CO is liberated per mole of CORM-3. CORM-3 prepared in water is relatively stable and retains its ability to liberate CO after 24 hours at room temperature.[16] Previously, we have reported that CORM-3 increased the osteogenic differentiation of rat BMSCs in vitro,[17] and the same result was acquired in the periodontal ligament stem cells.[18] However, the effect of CORM-3 on rat BMSCs in vivo and the underlying molecular mechanism remain unclear. In the experiments of our research group, the gene sequencing result of CORM-3-stimulated periodontal ligament stem cells suggested that miR-195-5p was significantly down-expressed during osteogenic differentiation. As miRNAs are highly conserved, we hypothesized that miR-195-5p might be down-expressed in CORM-3-stimulated BMSCs also and involved in the osteogenic differentiation. In the present study, the CORM-3-stimulated osteogenic differentiation of rat BMSCs was further studied in vivo, and the molecular mechanism in the CORM-3-stimulated osteogenic differentiation of rat BMSCs was investigated in vitro.

# Materials and Methods

## Cell Culture and Identification

4–5 weeks old male Wistar rats were obtained from the Animal Experimental Center of Shandong University (Jinan, China). The present study was approved by the Ethics Committee of the School of Stomatology, Shandong University.

Rat BMSCs were isolated and cultured as previously described.[17] Briefly, after the rats were euthanized, the femur and tibia were removed and the bone marrow cavity was rinsed with α-minimum essential medium (α-MEM) (Hyclone, GE Healthcare Life Sciences, UT, USA) supplemented with 20% fetal bovine serum (FBS) (Gibco, Invitrogen, CA, USA) and 100 U/mL penicillin–streptomycin (Invitrogen). Bone marrow fluid was incubated at 37°C in an atmosphere containing 5% $CO_2$. The medium was changed every 3 days, non-adherent cells were discarded. When cells reached 80-90% confluence, they were sub-cultured in α-MEM supplemented with 10% FBS (control medium). Rat BMSCs of passage 3 were used in the following experiments.

For osteogenic induction, cells were cultured in the osteogenic medium (Cyagen, Guangdong, China) (osteogenic group). Cells in the control group were cultured in the control medium. Following 21-day culture, cells were fixed with 4% paraformaldehyde at 37°C for 30 min, then incubated with 0.1% (pH 4.2) alizarin red S (Beijing Solarbio Science & Technology Co., Ltd., Beijing, China) at 37°C for 10 min. After washing with phosphate buffered saline (PBS; Solarbio), samples were observed using the phase-contrast microscope to verify the presence of mineralized nodules.

For adipogenic induction, cells were cultured in the adipogenic medium as previously described.[17] Cells in the control group were cultured in the control medium. Following 21-day culture, cells were fixed as mentioned above. The cells were then incubated with oil red O (Solarbio) at 37°C for 30 min and observed using the phase-contrast microscopy.

For clonogenesis experiment, rat BMSCs were seeded at a density of 3 cells/$cm^2$ and cultured in control medium. Following 10-days culture, cells were fixed with 4% paraformaldehyde for 30 min, then stained with 0.1% crystal violet for 10 min at 37°C. After washing with the tri-distilled water, cell clone was observed using the phase-contrast microscope. More than 50 cells were regarded as one cell clone. The clone formation rate was calculated as the number of cell clone/the total number of seeded cells × 100%, and the average value of six samples was obtained.

For subsequent CORM-3-stimulated osteogenic differentiation experiments in vitro, cells were cultured in the osteogenic medium containing 200 μM CORM-3 (Sigma-Aldrich, Shanghai, China) (CORM-3 group).

## Establishment of Animal Models with Periodontal Bone Defect

Animal experiments were approved by the Ethics Committee of Hospital of Stomatology, Shandong University (Protocol Number: 20190504) and carried out according to the National Institutes of Health Guide for the Care and Use of Laboratory Animals (NIH Publications No. 8023, revised 1978). The periodontal bone defect, which was 3 mm length, 2 mm width and 1 mm depth, was made with dental drill at the buccal alveolar bone of mandibular first and second molar, under general anesthesia (1% pentobarbital sodium, 40 mg/kg). The 8 weeks old male Wistar rats were randomly divided into four groups: (a) collagen membranes (ZH-BIO, Yantai, China) with rat BMSCs were implanted into the defects, and the rats were injected with CORM-3 (10mg/Kg, dissolved in 0.9% sodium chloride solution) intraperitoneally; (b) collagen membranes were implanted into the defects, with CORM-3 injection intraperitoneally; (c) collagen membranes with rat BMSCs were implanted into the defects, and the rats were injected with 0.9% sodium chloride solution intraperitoneally; (d) collagen membranes were implanted into the defects, and with 0.9% sodium chloride solution injection intraperitoneally. After 3 weeks, the rats were sacrificed, the mandibles were harvested and fixed in 4% paraformaldehyde for the following experiments.

## Micro-Computational Tomography (Micro-CT) and Histological Analysis

The specimens were scanned by micro-CT (SCANCO Medical AG, Switzerland). CT analysis software (Evaluation V6.5–3, SCANCO Medical AG, Switzerland) was used to reconstruct the images for 3D visualization and analysis. The percentage of bone volume (bone volume/tissue volume, BV/TV), trabecular numbers (Tb.N), trabecular thickness (Tb.Th) and trabecular separation (Tb. Sp) were measured and calculated for the assessment of bone regeneration of the defects.

H&E staining and immunohistochemical staining with rabbit anti-rat Runx2 polyclonal antibody (cat no., ab23981, 1:100 dilution; Abcam, USA) were used according to the manufacturer's protocols, and then the Image-Pro Plus 6.0 software was used to assess and calculate the bone regeneration of the defects.

## Transfection

For the mechanism studied in vitro, the rat BMSCs were transfected with miR-195-5p mimics (GenePharma, Shanghai, China), miR-195-5p inhibitor (GenePharma), pcDNA3.1-Wnt3a (BioSune, Shanghai, China), Wnt3a siRNA (GenePharma) or their corresponding controls using Micropoly-transfecter Cell Reagent (Micropoly, Jiangsu, China) according to the manufacturer's instructions. 24 hours after transfection, the cell viabilities were measured as previously described.[17] Briefly, 10 μL cell counting Kit-8 (Dojindo Molecular Technologies, Inc., Beijing, China) was added to each well, and cells were incubated for further 2 hours at 37°C. Subsequently, absorbance at 450 nm was measured using SPECTROstar Nano ultraviolet spectrophotometer (Spectro Analytical Instruments GmbH, Kleve, Germany). For the evaluation of transfection efficiency, after 24 hours transfection, the medium was replaced with control medium. 48 hours after transfection, cells were harvested for miR-195-5p and Wnt3a measurement. For subsequent osteogenic differentiation experiments, after 24 hours transfection, the medium was completely replaced with the osteogenic medium containing 200 μM CORM-3. In rescue experiment, cells were co-transfected with miR-195-5p mimics and pcDNA3.1-Wnt3a or miR-195-5p mimics and vector NC. For miR-195-5p target gene experiment, after 24 hours transfection, the medium was completely replaced with control medium.

## Quantitative Real-Time PCR Analysis

The level of miR-195-5p after transfection and mRNA expressions of osteogenic-related genes runt-related transcription factor 2 (Runx2) and osteopontin (OPN) during osteogenic differentiation were evaluated by real-time quantitative reverse transcription polymerase chain reaction (RT-qPCR) as previously described.[17] The primer sequences used were as follows: Runx2, forward 5'-CAGACACAATCCTCCCCACC-3', and reverse 5'-GCCAGAGGCAGAAGTCAGAG-3'; OPN, forward 5'-TCAAGGTCATCCCAGTTGCC-3', and reverse 5'-GACTCATGGCTGGTCTTCCC-3'; β-actin, forward 5'-CTCTGTGTGGATTGGTGGCT-3', and reverse 5'-CGCAGCTCAGTAACAGTCCG-3'; miRNA-195-5p, forward 5'-CGTTATCCTAGCAGCACAGAAAT-3', and reverse 5'-TATGGTTTTGACGACTGTGTGAT-3'; and U6, forward 5'-CAGCACATATACTAAAATTGGAACG-3', and reverse 5'-ACGAATTTGCGTGTCATCC-3'. Each sample was tested in triplicate, and the relative gene expressions were calculated using the $2^{-\Delta\Delta CT}$ method, with β-actin or U6 for normalization.

## Western Blot Analysis

Protein lysates were generated with radio immunoprecipitation assay lysis buffer (Solarbio). Then, protein concentrations were determined using BCA protein assay kit (Boster Biological Technology Co., Ltd., Wuhan, China) according to the manufacturer's protocol. Protein samples (20 μg/lane) were loaded onto 12% sodium dodecyl sulphate-polyacrylamide gel electrophoresis (SDS-PAGE) gel (Boster) and electrotransferred to a polyvinylidene fluoride (PVDF) membrane (Pall Corporation, Port Washington, NY, USA). After blocking with 5% non-fat milk, membranes were incubated overnight at 4°C with primary antibodies: rabbit anti-rat Runx2 monoclonal antibody (cat no., 12556s, 1:1000 dilution; Cell Signaling Technology, Inc., Danvers, MA, USA), rabbit anti-rat OPN polyclonal antibody (cat no., ab8448, 1:1000 dilution; Abcam, Cambridge, Britain), and rabbit anti-rat Wnt3a polyclonal antibody (cat no., WL0199a, 1:400 dilution; Wanleibio, Shenyang, China), respectively. Then, membranes were incubated with horseradish peroxidase-conjugated goat anti-rabbit secondary antibody (cat no., SA00001-2, 1:10,000 dilution; Proteintech Group, Inc., Rosemont, IL, USA) for 1 h at room temperature. Membranes were visualized by enhanced chemiluminescence (Amersham Pharmacia Biotech; Little Chalfont, U.K.). Loading differences were normalized using rabbit anti-rat GAPDH monoclonal antibody (cat no., CW0100, 1:2000 dilution; Beijin ComWin Biotech Co., Ltd., Beijing, China) or rabbit anti-rat Tubulin polyclonal antibody (cat no., 11224-1-AP, 1:1000 dilution; Proteintech). Protein band densities on scanned films were quantified using ImageJ 1.48u software (National Institutes of Health, Bethesda, MD, USA) and compared with the control.

## Analysis of Mineralization

Following 14-day culture, cells were fixed, then incubated with alizarin red S as mentioned above. For further evaluation, staining was dissolved in 100 μM cetylpyridinium chloride (CPC) for 1 h at 37°C. The optical density (OD) value of the

staining dissolved CPC was measured at 562 nm using the ELISA plate reader. All experiments were repeated for three times and each experiment in triplicate.

## Dual-Luciferase Reporter Assay

A luciferase reporter assay was carried out using a Dual-Luciferase Reporter Assay System (Promega, WI, U.S.A.). A fragment of the Wnt3a 3′UTR containing the predicted binding site for miR-195-5p or the respective binding site of the mutant-type (mut) 3′UTR was inserted into the pmirGLO vector (Zorin, Shanghai, China). All the constructs were verified by DNA sequencing. The vector containing wild-type (wt) or mut was transfected into the 293T cells with or without the miR-195-5p mimics. 24–48 hours after transfection, the luciferase activity was detected using the Dual-Luciferase Reporter Assay System and normalized to Renilla activity.

## Statistical Analysis

All experiments were repeated for three times. Data were presented as the mean ± standard deviation. The significance of difference was assessed by one-way analysis of variance method using GraphPad Prism 5 software (GraphPad Software, Inc., La Jolla, CA, USA), followed by the Tukey's post hoc test. $P<0.05$ was considered to indicate a statistically significant difference.

# Results

## Cell Identification

Cells were cultured as previously described. The passage 3 cells were uniform in shape, fusiform mainly, and grew in whirlpool shape. Cells were induced to differentiate into osteoblasts and adipocytes in different induction mediums. Cells highly expressed MSC surface markers CD90 (98.8%) and CD44 (92.6%), lowly expressed hematopoietic surface markers CD45 (0.1%) and CD34 (0.1%). Cells were seeded at low density and cultured for 10 days. After crystal violet staining, cell clone was seen by the phase-contrast microscope, and the clone formation rate was 24.3 ± 2.78% (not showed).

## Effect of CORM-3 and Rat BMSCs on Periodontal Bone Defect Repair in vivo

The surgical procedure is presented in Figure 1A. Collagen membranes (engrafted with or without BMSCs) were transplanted into the defect area. The bone regeneration was demonstrated by longitudinal micro-CT images and transverse X-ray image, as shown in Figure 1B. The results showed that collagen membranes with rat BMSC implantation in the presence of CORM-3 induced the most prominent bone regeneration among the four groups. The quantitative analysis of the region of interest (ROI) showed that the percentage of BV/TV in group (a) was increased by 1.61-, 2.23- and 5.65-fold, compared with group (b), (c) and (d), respectively ($P<0.05$). The Tb.N in group (a) and (b) were both significantly higher than that in group (d) ($P<0.05$); however, no significant difference was found between group (a) and (b) ($P>0.05$). The Tb.Th in all groups was roughly the same, no significant difference was found between any two groups ($P>0.05$). The Tb.Sp in group (a) was significantly lower than in other groups ($P<0.05$) (Figure 1C). Bone regenerative potential of CORM-3 on BMSCs was revealed by histological analysis. H&E staining showed that large amount of newly formed bone was observed in the surface of the bone defect in group (a). Very small amount of new bone was formed in group (b) and (c), and only scattered osteoid in group (d) in the surface of the bone defect was observed. The area ratio of newly formed bone in group (a) was increased by 3.35-, 4.07- and 12.67-fold, compared with group (b), (c) and (d), respectively ($P<0.05$) (Figure 1D). Immunohistochemical staining showed higher expression of Runx2 in the newly formed bone in group (a) than other groups, demonstrated by the highest integral optical density (IOD) in group (a) among all the groups. ($P<0.05$) (Figure 1E).

## Expression of miR-195-5p and wnt3a in the CORM-3-Stimulated Osteogenic Differentiation of Rat BMSCs

As indicated in Figure 2A, miR-195-5p level in cells cultured in COMR-3 group was obviously decreased compared with osteogenic group and control group after 24 hours ($P<0.05$). The protein expression of wnt3a was enhanced during the

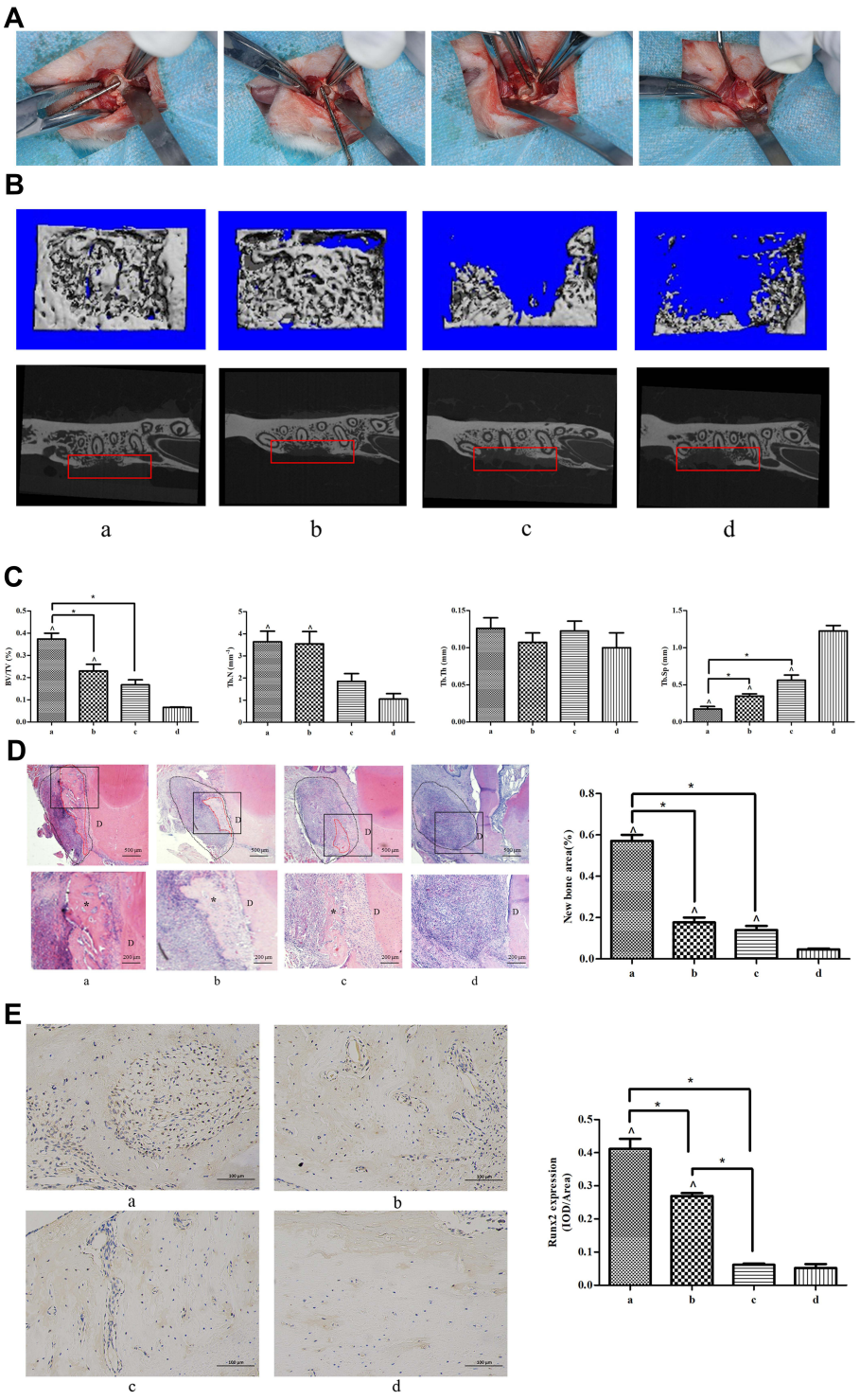


**Figure 1** Micro-CT and histological analysis of bone regeneration in periodontal bone defect in vivo. The rats were randomly divided into four groups: (a) collagen membranes with rat BMSCs were implanted into the defects, and the rats were injected with CORM-3 intraperitoneally; (b) collagen membranes were implanted into the defects, with CORM-3 injection intraperitoneally; (c) collagen membranes with rat BMSCs were implanted into the defects, and then the rats were injected with 0.9% sodium chloride solution intraperitoneally; (d) collagen membranes were implanted into the defects, with 0.9% sodium chloride solution injection intraperitoneally. (**A**) Photographs of the general surgical procedure. (**B**) The longitudinal Micro-CT images (upper panel) and transverse X-ray image (lower panel). Red frames were used to show the defect region with regeneration. (**C**) The quantitative analysis of the newly formed bone by CT analysis software. (**D**) H&E staining images of the newly formed bone under different magnifications. The staining image with the whole bone defect zone was labeled by the black dot line and the newly formed bone by the red dot line. The area within the black square was magnified and shown in the lower panel. "D" indicates the dentin. The black asterisk indicates the newly formed bone. The quantitative analysis of the newly formed bone by H&E staining was calculated using Image-Pro Plus 6.0 software. (**E**) Immunohistological images of newly formed bone by immunohistochemical staining of Runx2. Quantitative analyses of Runx2 expression using Image-Pro Plus 6.0 software. ^ $P<0.05$ vs control; * $P<0.05$ as indicated.

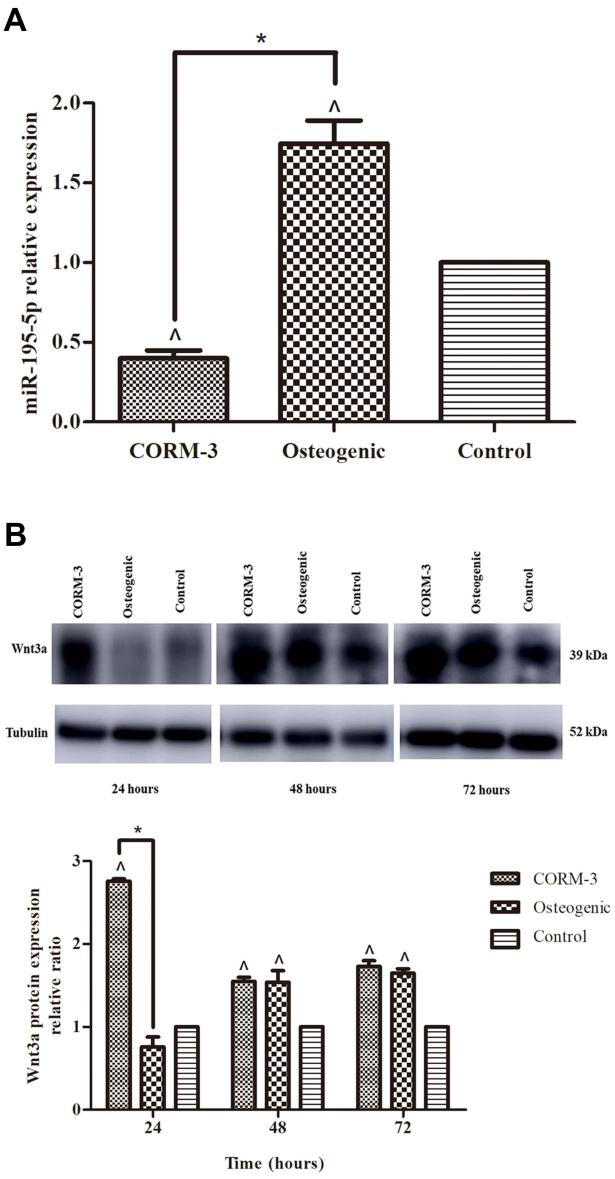


**Figure 2** Expressions of miR-195-5p and Wnt3a during osteogenic differentiation of rat BMSCs. Rat BMSCs in the CORM-3 or osteogenic group were cultured in the osteogenic medium with or without 200 μM CORM-3, respectively. Rat BMSCs in the control group were cultured in the control medium. (**A**) RT-qPCR analysis of miR-195-5p on 24 hours, normalized to U6. (**B**) Representative Western blot images of three independent experiments for Wnt3a protein expression at 24, 48 and 72 hours and quantitative results of Western blot images, using ImageJ software, normalized to Tubulin. The experiment was repeated for three times. Data were presented as the mean ±standard deviation (n=3). ^ $P<0.05$ vs control; * $P<0.05$ as indicated.

CORM-3-stimulated osteogenic differentiation of rat BMSCs (Figure 2B). At 24 hours, the protein expression of wnt3a in the COMR-3 group was increased by 3.63 and 2.76-fold compared with the osteogenic group and control group, respectively ($P<0.05$).

## CORM-3-Stimulated Osteogenic Differentiation of Rat BMSCs Was Modified by Up- or Down-Regulation of miR-195-5p

A successful transfection with miR-195-5p mimics and inhibitor was verified by RT-qPCR, and no significant difference in cell viability was found between any transfection group and control group ($P>0.05$) (Figure 3A). The mRNA expression of the Runx2 and OPN was assessed by RT-qPCR at different time points during osteogenic differentiation. With the overexpression of miR-195-5p, mRNA levels of both Runx2 and OPN were significantly

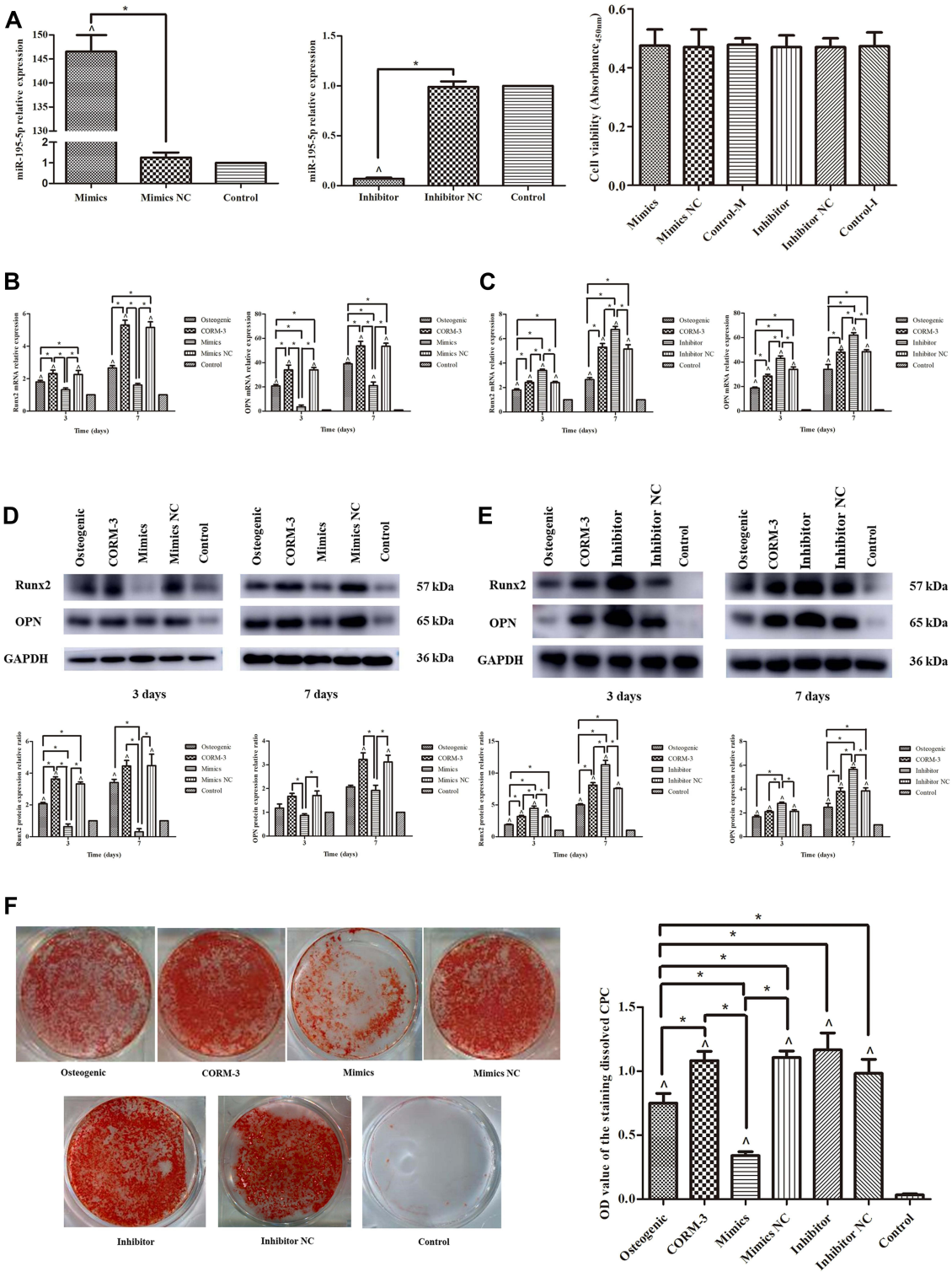


**Figure 3** CORM-3-stimulated osteogenic differentiation of rat BMSCs was modified by up- or down-regulation of miR-195-5p. (**A**) The rat BMSCs were transfected with miR-195-5p mimics and inhibitor. 24 hours after transfection, the cell viabilities were measured. After 48 hours, the expressions of miR-195-5p were determined by RT-qPCR, normalized to U6. (**B** and **C**) The rat BMSCs were transfected with miR-195-5p mimics and mimics NC (**B**), miR-195-5p inhibitor and inhibitor NC (**C**) for 24 hours and then cultured in the osteogenic medium containing 200 μM CORM-3. Meanwhile, cells in the osteogenic, CORM-3 or control group were cultured in the osteogenic medium, osteogenic medium containing 200 μM CORM-3 or control medium respectively. After 3 and 7 days, the mRNA expressions of Runx2 and OPN were determined by RT-qPCR, normalized to β-actin. (**D** and **E**) The rat BMSCs were cultured as B and C described above. After 3 and 7 days, the protein expressions of Runx2 and OPN were determined by Western blot, then analysed using ImageJ software, normalized to GAPDH. (**F**) The rat BMSCs were cultured in different mediums as described above. After 14 days, the mineralization was determined by alizarin red staining and semi quantitative analysis. The experiment was repeated for three times. Data were presented as the mean±standard deviation (n=3). ^ $P<0.05$ vs control; * $P<0.05$ as indicated.

lower than that in the CORM-3 group on the 3rd and 7th day of osteogenic induction ($P<0.05$) (Figure 3B). When miR-195-5p was inhibited, the mRNA expressions of Runx2 and OPN were increased by 1.4- and 1.5-fold, respectively, on the 3rd day ($P<0.05$), and both 1.3-fold on the 7th day of osteogenic induction, compared with CORM-3 group ($P<0.05$) (Figure 3C). In consistence with the mRNA expressions, the protein expressions of Runx2 and OPN in the CORM-3-stimulated osteogenic differentiation were significantly decreased in miR-195-5p over-expressed cells, but increased in miR-195-5p deficient cells ($P<0.05$) (Figures 3D and E). The results from the alizarin red staining and semi-quantitative analysis demonstrated that the mineralization was decreased significantly ($P<0.05$) on the 14th day of osteogenic differentiation when miR-195-5p was overexpressed. However, the increased effect was not observed in miR-195-5p-deficient cells (Figure 3F).

## miR-195-5p Directly Targeted Wnt3a

TargetScan, miRanda and miRBase were utilized to predict the potential target genes of miR-195-5p. Among them, Wnt3a had a miR-195-5p-binding site in their 3′UTR (Figure 4A). After up-regulation and down-regulation of miR-195-5p level in cells, the protein expression of Wnt3a was decreased and increased correspondingly ($P<0.05$) (Figures 4B and C). In order to test whether miR-195-5p directly targets Wnt3a, dual-luciferase reporter assay was constructed, which had either the Wnt3a 3′UTR-wt or the Wnt3a 3′UTR-mut (Figure 4A). The miR-195-5p mimics restrained the luciferase reporter activity of the Wnt3a 3′UTR-wt by 19% ($P<0.05$); however, the activity was markedly increased with the Wnt3a 3′UTR-mut and miR-195-5p mimics co-transfection ($P<0.05$) (Figure 4D).

## CORM-3-Stimulated Osteogenic Differentiation of Rat BMSCs Was Modified by Up- or Down-Regulation of Wnt3a

A successful transfection with pcDNA3.1-Wnt3a or Wnt3a siRNA was confirmed by Western blotting analysis, and no significant difference in cell viability was found between any transfection group and control group ($P>0.05$) (Figure 5A). With overexpression of Wnt3a, the mRNA levels of Runx2 and OPN were increased by 1.34- and 1.82-fold, respectively, on the 3rd day ($P < 0.05$), and 1.40- and 1.29-fold, respectively, on the 7th day of osteogenic induction, compared with CORM-3 group ($P<0.05$) (Figure 5B). On the contrary, in Wnt3a-deficient cells, mRNA expressions of Runx2 and OPN were all reduced on the 3rd and the 7th day of osteogenic induction ($P<0.05$) (Figure 5C). The protein expressions of Runx2 and OPN during the osteogenic induction were also increased or decreased with up- or down-regulation of Wnt3a. In Wnt3a-overexpressed cells, the protein expressions of Runx2 and OPN were increased by 1.60- and 1.85-fold, respectively, on the 3rd day, 2.02- and 2.56-fold, respectively, on the 7th day of osteogenic induction, compared with CORM-3 group ($P<0.05$) (Figures 5D and E). Moreover, mineralization in Wnt3a-overexpressed cells was enhanced significantly on the 14th day of osteogenic induction, compared with CORM-3 group ($P<0.05$). The opposite effect was observed in Wnt3a-deficient cells ($P<0.05$) (Figure 5F).

## Decreased Osteogenic Differentiation Capacity by miR-195-5p Up-Regulation Was Rescued with Wnt3a Overexpression

To prove whether the effect of miR-195-5p depended on the expression of Wnt3a during CORM-3-stimulated osteogenic differentiation, rat BMSCs were co-transfected with miR-195-5p mimics and pcDNA3.1-Wnt3a. With the increased expression of miR-195-5p, the mRNA and protein expressions of Runx2 and OPN on the 3rd and 7th day of osteogenic differentiation and the matrix mineralization on the 14th day were rescued with Wnt3a overexpression, rebounding to the level of CORM-3 group. Especially, the mRNA expression of Runx2 on the 7th day in miR-195-5p mimics and pcDNA3.1-Wnt3a co-transfection group was obviously raised compared with that in COMR-3 group ($P<0.05$) (Figure 6).

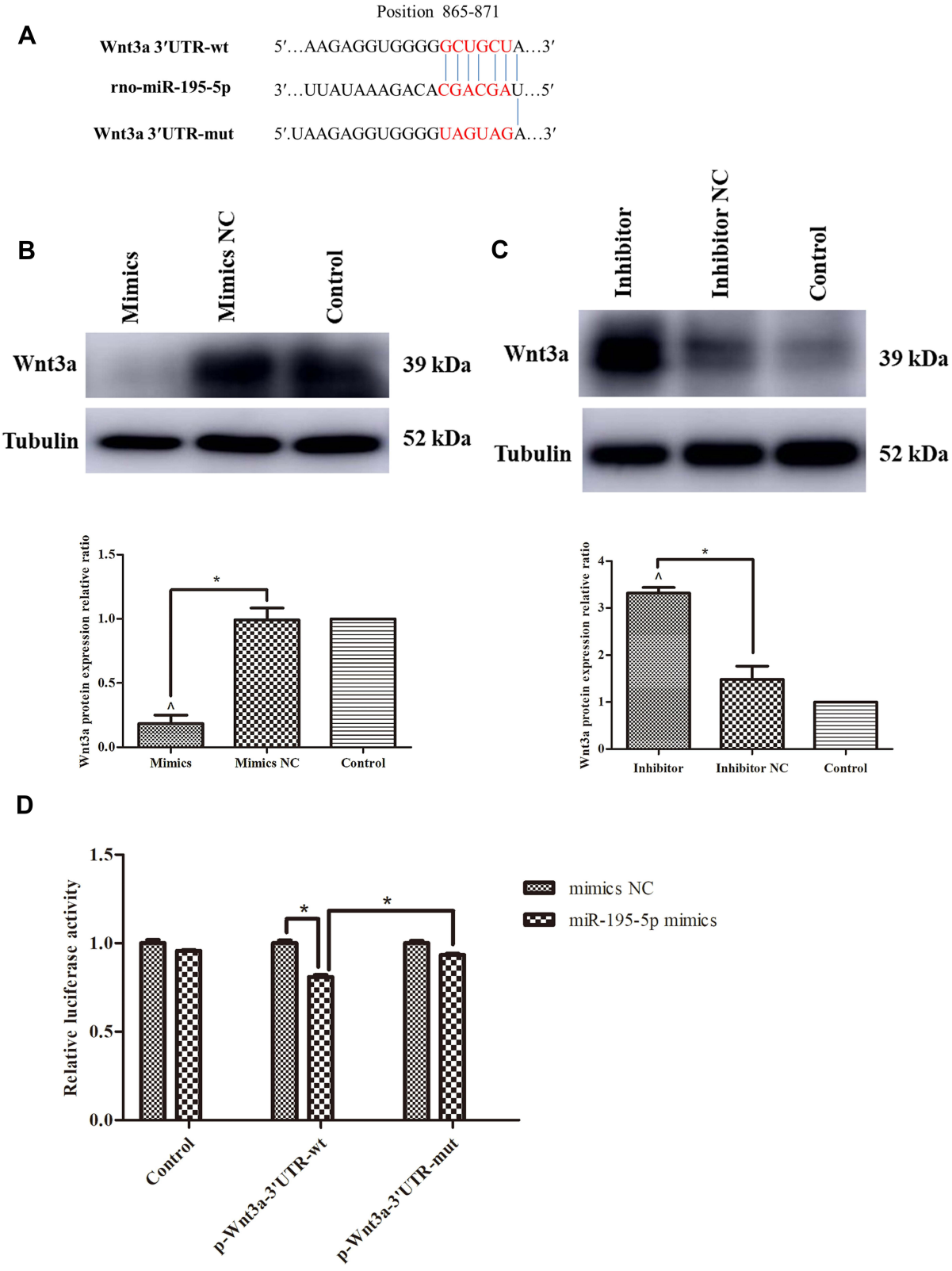


**Figure 4** miR-195-5p directly targeted Wnt3a. (**A**) The design of luciferase reporters with Wnt3a 3′UTR-wt or Wnt3a 3′UTR-mut, the position also showed. (**B** and **C**) Western blot images and analysis for Wnt3a protein expression in rat BMSCs after 48 hours transfection with miR-195-5p mimics or mimics NC (**B**), miR-195-5p inhibitor or inhibitor NC (**C**), using ImageJ software, normalized to Tubulin. (**D**) Effect of miR-195-5p mimics on luciferase activity in 293T cells transfected with either the 3′UTR-wt reporter or the 3′UTR-mut reporter for Wnt3a. The experiment was repeated for three times. Data were presented as the mean±standard deviation (n=3). ^ $P<0.05$ vs control; * $P<0.05$ as indicated.

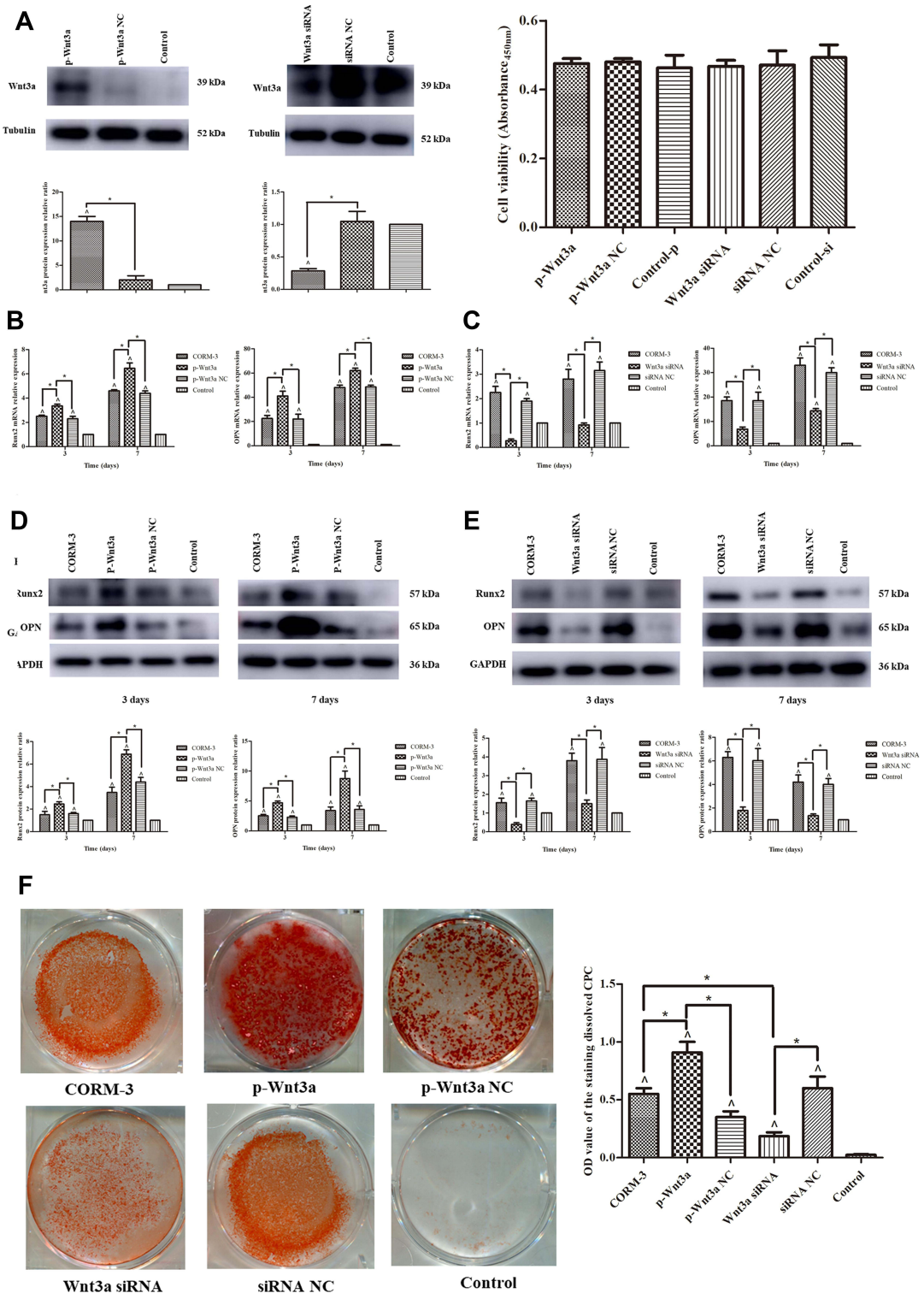


**Figure 5** CORM-3-stimulated osteogenic differentiation of rat BMSCs was modified by up- or down-regulation of Wnt3a. (**A**) The rat BMSCs were transfected with pcDNA3.1-Wnt3a and Wnt3a siRNA. 24 hours after transfection, the cell viabilities were measured. After 48 hours, the protein expressions of Wnt3a were determined by Western blot and image analysis. (**B** and **C**) The rat BMSCs were transfected with pcDNA3.1-Wnt3a or NC (**B**), Wnt3a siRNA or NC (**C**) for 24 hours and then cultured in the osteogenic medium containing 200 μM CORM-3. Meanwhile, cells in the CORM-3 or control group were cultured in the osteogenic medium containing 200 μM CORM-3 or control medium respectively. After 3 and 7 days, the mRNA expressions of Runx2 and OPN were determined by RT-qPCR, normalized to β-actin. (**D** and **E**) The rat BMSCs were cultured as B and C described above. After 3 and 7 days, the protein expressions of Runx2 and OPN were determined by Western blot, then analysed using ImageJ software, normalized to GAPDH. (**F**) The rat BMSCs were cultured in different mediums as described above. After 14 days, the mineralization was determined by alizarin red staining and semi quantitative analysis. The experiment was repeated for three times. Data were presented as the mean±standard deviation (n=3). ^ $P<0.05$ vs control; * $P<0.05$ as indicated.

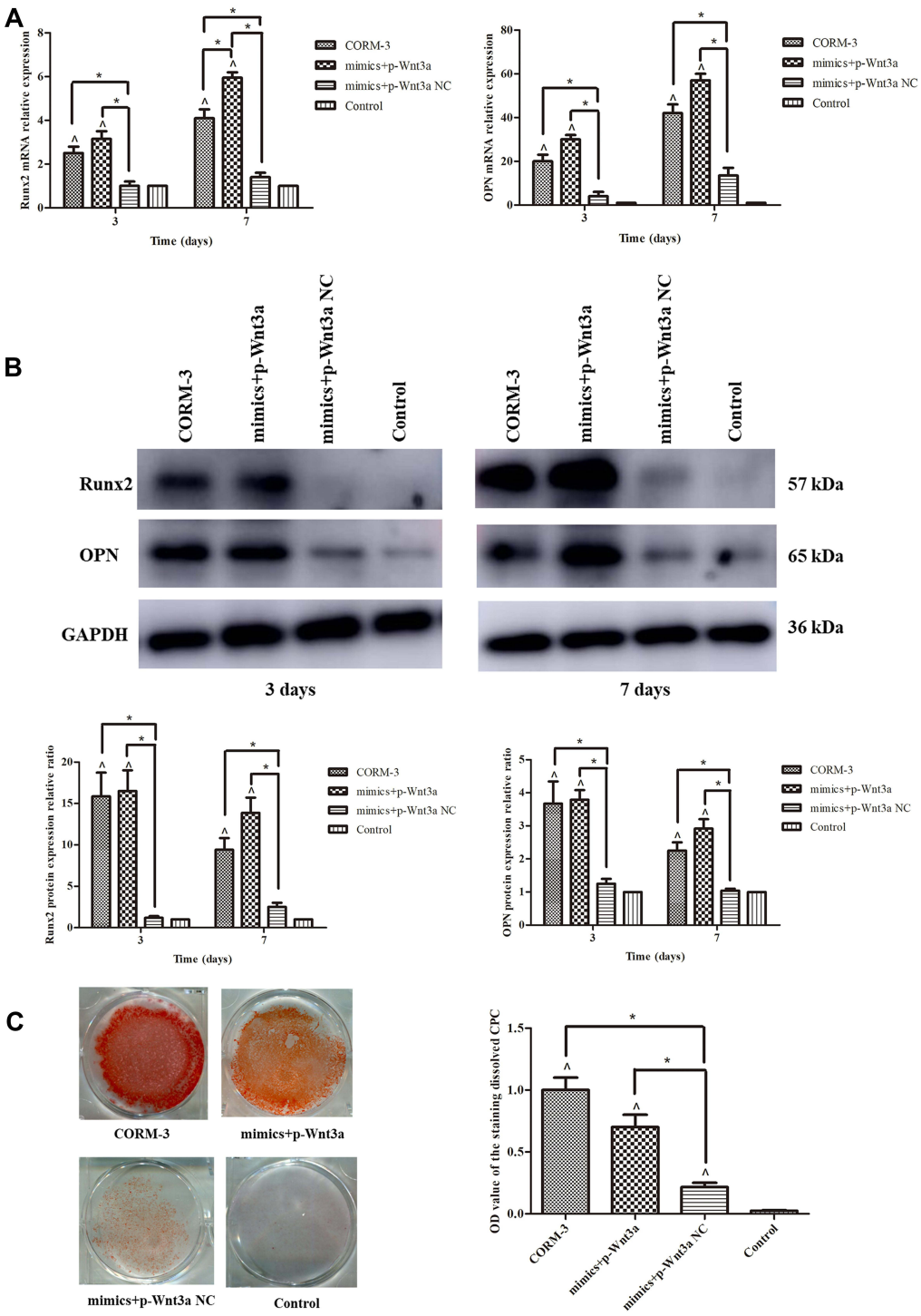


**Figure 6** Decreased osteogenic differentiation capacity by miR-195-5p up-regulation was rescued with Wnt3a overexpression. (**A**) The rat BMSCs were co-transfected with miR-195-5p mimics and pcDNA3.1-Wnt3a, miR-195-5p mimics and NC for 24 hours and then cultured in the osteogenic medium containing 200 μM CORM-3. Meanwhile, cells in the CORM-3 or control group were cultured in the osteogenic medium containing 200 μM CORM-3 or control medium respectively. After 3 and 7 days, the mRNA expressions of Runx2 and OPN were determined by RT-qPCR, normalized to β-actin. (**B**) The rat BMSCs were cultured in different mediums as described above. After 3 and 7 days, the protein expressions of Runx2 and OPN were determined by Western blot, then analysed using ImageJ software, normalized to GAPDH. (**C**) The rat BMSCs were cultured in different mediums as described above. After 14 days, the mineralization was determined by alizarin red staining and semi quantitative analysis. The experiment was repeated for three times. Data were presented as the mean±standard deviation (n=3). ^ $P<0.05$ vs control; * $P<0.05$ as indicated.

## Discussion

Bone defects caused by trauma, tumor and inflammation disease seriously reduce the quality of life of patients. Stem cell-based engineering has come to the fore as a hopeful and promising approach to bone regeneration.[1,4] BMSCs are currently considered as the gold standard cell source for bone tissue engineering, because of their self-renewal and multipotential differentiation capacity.[2,3,19] Lee et al reported that BMSCs exhibited high bone regeneration efficacy in rabbit calvarial defects.[20] In the study of dog mandibular defects, BMSCs manifested strong osteogenic potential, as significantly more new bone was formed in the BMSC groups than otherwise.[21] Multiple biological materials and growth factors have been implemented for osteoinduction of BMSCs.[22,23] CORMs, a novel group of compounds that can sustainedly release CO,[24] have exhibited such potent effects as anti-inflammatory,[25] anti-apoptotic,[26] neuroprotective,[27] vascular function improvement and so on.[24,28] Our previous study showed that CORM-3 promoted the osteogenic differentiation of rat BMSCs in vitro.[17] In this study, the periodontal defects treated with CORM-3-stimulated rat BMSC transplant achieved better bone repair and regeneration. These results suggested CORM-3 had great potential in the treatment of periodontal disease and other bone defect diseases.

miRNAs, about 22 nucleotides in length, are highly conserved endogenous RNAs. miRNAs can lead to translational silence by binding to the 3′UTR of target mRNAs, thus regulating cell proliferation, differentiation, apoptosis, and so on.[7,11,29] Many studies have demonstrated that miRNAs play a key role in the osteogenic differentiation of BMSCs.[11–14] Recently, researchers have uncovered CORM mechanism associated with miRNAs.[30] CORM-2 prevents TNF-α-induced endothelial nitric oxide synthase downregulation by inhibiting miR-155-5p biogenesis.[31] CORM-3 ameliorates structural and functional cardiac recovery after myocardial injury via decreasing miR-206 expression.[32] However, little is known about CORMs and miR-195-5p. In the present study, we first confirmed the down-expression of miR-195-5p in CORM-3-stimulated osteogenic differentiation of rat BMSCs, based on the previous gene sequencing result. Our results suggested that miR-195-5p might be involved in the CORM-3-stimulated osteogenic differentiation of rat BMSCs.

Runx2 is an osteogenesis-specific transcription factor and has an important impact on osteogenic differentiation of BMSCs.[33,34] As a marker for early osteogenic differentiation, it can promote the expressions of a number of downstream genes associated with osteogenic differentiation.[35] OPN is a multifunctional protein mainly associated with bone formation. OPN is secreted by osteoblast and is a characteristic phenotypic marker of osteoblast. It is stored in bone matrix and affects the matrix mineralization.[36,37] In the present study, the CORM-3-stimulated osteogenic differentiation of rat BMSCs was suppressed by overexpression of miR-195-5p, evidenced by the results of decreased mRNA and protein expressions of Runx2 and OPN, and matrix mineralization demonstrated. Meanwhile, the expressions of osteogenic related factors during the CORM-3-stimulated osteogenic differentiation were enhanced by down-regulation of miR-195-5p. These results suggested that miR-195-5p might be involved in the CORM-3-stimulated osteogenic differentiation. However, from our experiment, the matrix mineralization was not enhanced significantly in miR-195-5p-deficient cells. This discrepancy might be due to the following considerations. First, the mechanism underlying CORM-3-stimulated osteogenic differentiation is complex. Though the alizarin red staining of the mimics group was evidently decreased than that in the CORM-3 group, the scattered spots of alizarin red staining were still seen, which was obviously enhanced than that in the control group. It suggested that there might have other mechanisms involved in the CORM-3-stimulated osteogenic differentiation of rat BMSCs. Secondly, miRNAs are complex network structure. Inhibition of miR-195-5p expression via transfection in vitro might affect the levels of other miRNAs, which led to compensatory converse effect on osteogenic differentiation.

For further research, we first predicted the potential target gene Wnt3a of miR-195-5p by bioinformatics software. In the following experiment, up-regulation of miR-195-5p level decreased the protein expression of Wnt3a in cells. Conversely, the protein expression of Wnt3a was enhanced in miR-195-5p-deficient cells. According to the gene homology analysis, it is estimated to comprise 66–82% of the conserved regions between rat and human.[38] The genes between human and rat are highly homologous, and the binding targets between miRNAs and mRNA are evolutionarily conserved. Additionally, position 1426–1432 of human Wnt3a 3’ UTR and position 865–871 of rat Wnt3a 3’ UTR are both targeted with miR-195-5p, based on the target gene prediction software. Therefore, human 293T cells were used for

dual-luciferase experiment. The results from the luciferase reporter assay, together with the data on the regulatory effect of miR-195-5p on Wnt3a, demonstrated that miR-195-5p directly targeted Wnt3a.

The Wnt signaling pathway plays a vital role in osteogenesis, and it is strongly implicated in skeletal tissue regeneration and repair.[39,40] Activation of the Wnt signaling pathway promotes the osteogenic differentiation of BMSCs in vitro.[41,42] Wnt signaling pathway is involved in the process of promoting fracture healing of rats with nonunion in vivo.[43] The Wnt ligands can bind receptors on the surface of cells, then activate the Wnt pathway. During the fracture healing process, the expressions of many Wnt ligands and receptors are upregulated.[39] Wnts now comprise a family of secreted glycoproteins, in which Wnt3a is included.[44,45] Wnt3a can enhance cell survival and reestablish the osteogenic capacity of bone grafts from aged animals, resulting in significantly more osseous regeneration.[46] Wnt3a signaling induces murine dental follicle cells to differentiate into cementoblastic/osteoblastic cells.[47] Some miRNAs specifically interact with Wnt ligands, leading to subsequent regulation of osteogenic differentiation.[48,49] Upregulation of miR-16-2* blocks the Wnt signal pathway by targeting Wnt5a directly. miR-16-2* interferes with Wnt5a to regulate osteogenic differentiation of human BMSCs.[50] miR-196a promotes osteogenic differentiation of adipose stem cells by modulating Wnt/β-catenin pathway.[51] Based on our study, in BMSCs miR-195-5p targets Wnt3a. Moreover, Wnt3a is a known target of miR-195 in other tissues and diseases. MiR-195 suppresses the proliferation, migration, and invasion of colon cancer by targeting Wnt3a.[52] MiR-195 is key in regulating cell proliferation, cell cycle and apoptosis through directly targeting Wnt3a and acts as a tumor suppressor in HepG2 hepatocellular carcinoma cells.[53] MiR-195-5p regulates osteogenic differentiation of periodontal ligament cells by targeting Wnt3a.[54] Therefore, we hypothesized the involvement of Wnt3a in the osteogenesis of rat BMSCs. As shown in the present study, the protein expression of Wnt3a was enhanced during the CORM-3-stimulated osteogenic differentiation of rat BMSCs. Moreover, CORM-3-stimulated osteogenic differentiation was enhanced by Wnt3a overexpression, with the increased mRNA and protein expressions of Runx2 and OPN, and matrix mineralization. In contrast, the CORM-3-stimulated osteogenic differentiation was suppressed in the Wnt3a-deficient cells. These results suggested that Wnt3a, as the target of miR-195-5p, was involved in the CORM-3-stimulated osteogenic differentiation of rat BMSCs.

As the data shown, the CORM-3-stimulated osteogenic differentiation was decreased in cells transfected with miR-195-5p mimics. To further verify the role of miR-195-5p/Wnt3a pathway in CORM-3 induced osteogenic differentiation, rescue experiments were conducted by co-transfection. The decreased osteogenic differentiation capacity was rescued by miR-195-5p mimics and pcDNA3.1-Wnt3a co-transfection. The miR-195-5p/Wnt3a was presented as an obvious link between CORM-3 and osteogenic differentiation in rat BMSCs.

CO, as a gasotransmitter, has showed many physiological roles in different organs and tissues. CO administration has therapeutic potential in many diseases.[32,55,56] CO has already been evaluated in Phase I clinical testing and the feasibility and anti-inflammatory effects of low-dose CO inhalation in patients with chronic obstructive pulmonary disease have been proved. Patients inhaled 100–125 ppm CO for 2 hours on 4 consecutive days is well tolerated, feasible and safe.[57] Mishra S et al reported that 1000 ppm CO inhalation for 16 h rescues ischemic lungs by interrupting MAPK-driven expression of early growth response 1 gene and its downstream target genes.[58] The recent observations that CO inhalation (500 ppm for 1 h) at various time points after injection of a lethal dose of endotoxin rescues 20–90% of mice from fulminant hepatitis emphasize the potential importance of CO therapy in an intensive care setting.[59] The data reported so far in the literature indicate that a 15–20% proportion of HbCO is, in the majority of cases, not detrimental and can be considered the "biological threshold" for CO tolerance in humans beyond which severe CO-mediated injury is likely to occur.[60] The toxicity and limitation of CO gas prevented the CO application. CORMs, capable of liberating controlled quantities of CO, have been a valid alternative.[15] CORMs, with great potential in in vivo biosafety, have shown a variety of pharmacological activities, with numerous reports on the biological applications of CORMs in inflammatory, vascular disease, organ transplantation and cancer.[24,55,61,62] CORMs, as a new type of drugs, have tremendous therapeutic potential, and may become a new class of therapeutics against various diseases.[63]

## Conclusions

In summary, the present study indicates that carbon monoxide-releasing molecule-3 promotes osteogenic differentiation of rat BMSCs via miRNA-195-5p/Wnt3a pathway. Our results provide a new molecular mechanism for CORMs, boding well for the application of CORM-3 in the treatment of periodontal disease and other bone-defect diseases.

## Abbreviations

BMSCs, bone marrow-derived mesenchymal stem cells; CORM, carbon monoxide releasing molecule; CPC, cetylpyridinium chloride; FBS, fetal bovine serum; miRNAs, microRNAs; mut, mutant-type; OD, optical density; OPN, osteopontin; PBS, phosphate buffered saline; PVDF, polyvinylidene fluoride; RT-qPCR, real-time quantitative reverse transcription polymerase chain reaction; Runx2, runt-related transcription factor 2; SDS-PAGE, sodium dodecyl sulphate-polyacrylamide gel electrophoresis; UTR, untranslated region; wt, wild-type; α-MEM, α-minimum essential medium.

## Ethics Approval and Consent to Participate

All guidelines on animal care and use applicable to international, national and/or institutions have been complied with.

## Acknowledgments

The present study was supported by Shandong Provincial Natural Science Foundation (ZR2020MH186), Shandong Provincial Science and Technology Development Plan (2010GSF10270).

## Disclosure

The authors declare no conflicts of interest in this work.

## References

1. Luby AO, Ranganathan K, Lynn JV, Nelson NS, Donneys A, Buchman SR. Stem cells for bone regeneration: current state and future directions. *J Craniofac Surg*. 2019;30(3):730–735. doi:10.1097/SCS.0000000000005250
2. Dai F, Du P, Chang Y, et al. Downregulation of miR-199b-5p inducing differentiation of bone-marrow mesenchymal stem cells (BMSCs) toward cardiomyocyte-like cells via HSF1/HSP70 pathway. *Med Sci Monit*. 2018;24:2700–2710. doi:10.12659/MSM.907441
3. Jing W, Zuo D, Cai Q, et al. Promoting neural transdifferentiation of BMSCs via applying synergetic multiple factors for nerve regeneration. *Exp Cell Res*. 2019;375(2):80–91. doi:10.1016/j.yexcr.2018.12.021
4. Polymeri A, Giannobile WV, Kaigler D. Bone marrow stromal stem cells in tissue engineering and regenerative medicine. *Horm Metab Res*. 2016;48(11):700–713. doi:10.1055/s-0042-118458
5. Bartel DP. MicroRNAs: genomics, biogenesis, mechanism, and function. *Cell*. 2004;116(2):281–297. doi:10.1016/s0092-8674(04)00045-5
6. Mohr AM, Mott JL. Overview of microRNA biology. *Semin Liver Dis*. 2015;35(1):3–11. doi:10.1055/s-0034-1397344
7. O'Brien J, Hayder H, Zayed Y, Peng C. Overview of MicroRNA biogenesis, mechanisms of actions, and circulation. *Front Endocrinol*. 2018;9:402–413. doi:10.3389/fendo.2018.00402
8. Vimalraj S, Selvamurugan N. MicroRNAs: synthesis, gene regulation and osteoblast differentiation. *Curr Issues Mol Biol*. 2013;15:7–18.
9. Hata A, Kang H. Functions of the bone morphogenetic protein signaling pathway through microRNAs (review). *Int J Mol Med*. 2015;35(3):563–568. doi:10.3892/ijmm.2015.2060
10. Zhang L, Tang Y, Zhu X, et al. Overexpression of miR-335-5p promotes bone formation and regeneration in mice. *J Bone Miner Res*. 2017;32(12):2466–2475. doi:10.1002/jbmr.3230
11. Wang J, Liu S, Li J, Zhao S, Yi Z. Roles for miRNAs in osteogenic differentiation of bone marrow mesenchymal stem cells. *Stem Cell Res Ther*. 2019;10(1):197. doi:10.1186/s13287-019-1309-7
12. Li B. MicroRNA regulation in osteogenic and adipogenic differentiation of bone mesenchymal stem cells and its application in bone regeneration. *Curr Stem Cell Res T*. 2018;13(1):26–30. doi:10.2174/1574888X12666170605112727
13. Li Y, Yang F, Gao M, et al. MiR-149-3p regulates the switch between adipogenic and osteogenic differentiation of BMSCs by targeting FTO. *Mol Ther Nucleic Acids*. 2019;17:590–600. doi:10.1016/j.omtn.2019.06.023
14. Huang Y, Hou Q, Su H, Chen D, Luo Y, Jiang T. miR488 negatively regulates osteogenic differentiation of bone marrow mesenchymal stem cells induced by psoralen by targeting Runx2. *Mol Med Rep*. 2019;20(4):3746–3754. doi:10.3892/mmr.2019.10613
15. Motterlini R, Mann BE, Johnson TR, Clark JE, Foresti R, Green CJ. Bioactivity and pharmacological actions of carbon monoxide-releasing molecules. *Curr Pharm Des*. 2003;9(30):2525–2539. doi:10.2174/1381612033453785
16. Clark JE, Naughton P, Shurey S, et al. Cardioprotective actions by a water-soluble carbon monoxide-releasing molecule. *Circ Res*. 2003;93(2):e2–8. doi:10.1161/01
17. Li J, Song L, Hou M, Wang P, Wei L, Song H. Carbon monoxide releasing molecule-3 promotes the osteogenic differentiation of rat bone marrow mesenchymal stem cells by releasing carbon monoxide. *Int J Mol Med*. 2018;41(4):2297–2305. doi:10.3892/ijmm.2018.3437
18. Chen H, Dai Y, Cui J, et al. Carbon monoxide releasing molecule-3 enhances osteogenic differentiation of human periodontal ligament stem cells by carbon monoxide release. *Drug Des Devel Ther*. 2021;15:1691–1704. doi:10.2147/DDDT.S300356
19. Fu X, Liu G, Halim A, Ju Y, Luo Q, Song AG. Mesenchymal stem cell migration and tissue repair. *Cells*. 2019;8(8):784. doi:10.3390/cells8080784
20. Lee YC, Chan YH, Hsieh SC, Lew WZ, Feng SW. Comparing the osteogenic potentials and bone regeneration capacities of bone marrow and dental pulp mesenchymal stem cells in a rabbit calvarial bone defect model. *Int J Mol Sci*. 2019;20(20):5015. doi:10.3390/ijms20205015
21. Wang F, Zhou Y, Zhou J, et al. Comparison of intraoral bone regeneration with iliac and alveolar BMSCs. *J Dent Res*. 2018;97(11):1229–1235. doi:10.1177/0022034518772283

22. Zhang H, Mao X, Du Z, et al. Three dimensional printed macroporous polylactic acid/hydroxyapatite composite scaffolds for promoting bone formation in a critical-size rat calvarial defect model. *Sci Technol Adv Mat*. 2016;17(1):136–148. doi:10.1080/14686996.2016.1145532
23. Um S, Kim HY, Seo B. Effects of BMP-2 on the osteogenic differentiation of bone marrow stem cells in fibrous dysplasia. *Oral Dis*. 2018;24 (6):1057–1067. doi:10.1111/odi.12869
24. Motterlini R, Clark JE, Foresti R, Sarathchandra P, Mann BE, Green CJ. Carbon monoxide-releasing molecules: characterization of biochemical and vascular activities. *Circ Res*. 2002;90(2):E17–24. doi:10.1161/hh0202.104530
25. Lee C, Wu C, Chiang Y, et al. Carbon monoxide releasing molecule-2 attenuates pseudomonas aeruginosa-induced ROS-dependent ICAM-1 expression in human pulmonary alveolar epithelial cells. *Redox Biol*. 2018;18:93–103. doi:10.1016/j.redox.2018.07.001
26. Ulbrich F, Kaufmann KB, Meske A, et al. The CORM ALF-186 mediates anti-apoptotic signaling via an activation of the p38 MAPK after ischemia and reperfusion injury in retinal ganglion cells. *PLoS One*. 2015;11:e165182. doi:10.1371/journal.pone.0165182
27. Ulbrich F, Hagmann C, Buerkle H, et al. The carbon monoxide releasing molecule ALF-186 mediates anti-inflammatory and neuroprotective effects via the soluble guanylate cyclase β1 in rats' retinal ganglion cells after ischemia and reperfusion injury. *J Neuroinflammation*. 2017;14(1):130. doi:10.1186/s12974-017-0905-7
28. Foresti R, Hammad J, Clark JE, et al. Vasoactive properties of CORM-3, a novel water-soluble carbon monoxide-releasing molecule. *Brit J Pharmacol*. 2004;142(3):453–460. doi:10.1038/sj.bjp.0705825
29. Jackson RJ, Standart N. How do microRNAs regulate gene expression? *Sci STKE*. 2007;2007(367):re1. doi:10.1126/stke.3672007re1
30. Uchiyama K, Naito Y, Takagi T, et al. Carbon monoxide enhance colonic epithelial restitution via FGF15 derived from colonic myofibroblasts. *Biochem Bioph Res Co*. 2010;391(1):1122–1126. doi:10.1016/j.bbrc.2009.12.035
31. Choi S, Kim J, Kim J, et al. Carbon monoxide prevents TNF-alpha-induced eNOS downregulation by inhibiting NF-kappaB-responsive miR-155-5p biogenesis. *Exp Mol Med*. 2017;49(11):e403. doi:10.1038/emm.2017.193
32. Segersvard H, Lakkisto P, Hanninen M, et al. Carbon monoxide releasing molecule improves structural and functional cardiac recovery after myocardial injury. *Eur J Pharmacol*. 2018;818:57–66. doi:10.1016/j.ejphar.2017.10.031
33. Xu J, Li Z, Hou Y, Fang W. Potential mechanisms underlying the Runx2 induced osteogenesis of bone marrow mesenchymal stem cells. *Am J Transl Res*. 2015;7(12):2527–2535.
34. Komori T, Yagi H, Nomura S, et al. Targeted disruption of Cbfa1 results in a complete lack of bone formation owing to maturational arrest of osteoblasts. *Cell*. 1997;89(5):755–764. doi:10.1016/s0092-8674(00)80258-5
35. Deng Y, Wu S, Zhou H, et al. Effects of a miR-31, Runx2, and Satb2 regulatory loop on the osteogenic differentiation of bone mesenchymal stem cells. *Stem Cells Dev*. 2013;22(16):2278–2286. doi:10.1089/scd.2012.0686
36. De Fusco C, Messina A, Monda V, et al. Osteopontin: relation between adipose tissue and bone homeostasis. *Stem Cells Int*. 2017;2017:4045238. doi:10.1155/2017/4045238
37. Singh A, Gill G, Kaur H, Amhmed M, Jakhu H. Role of osteopontin in bone remodeling and orthodontic tooth movement: a review. *Prog Orthod*. 2018;19(1):18. doi:10.1186/s40510-018-0216-2
38. Nilsson S, Helou K, Walentinsson A, Szpirer C, Nerman O, Ståhl F. Rat-mouse and rat-human comparative maps based on gene homology and high-resolution zoo-FISH. *Genomics*. 2001;74(3):287–298. doi:10.1006/geno.2001.6550
39. Xu H, Duan J, Ning D, et al. Role of Wnt signaling in fracture healing. *Bmb Rep*. 2014;47(12):666–672. doi:10.5483/bmbrep.2014.47.12.193
40. Houschyar KS, Tapking C, Borrelli MR, et al. Wnt pathway in bone repair and regeneration – what do we know so far. *Front Cell Dev Biol*. 2019;6:170–182. doi:10.3389/fcell.2018.00170
41. Chen X, Shen Y, He M, et al. Polydatin promotes the osteogenic differentiation of human bone mesenchymal stem cells by activating the BMP2-Wnt/beta-catenin signaling pathway. *Biomed Pharmacother*. 2019;112:108746. doi:10.1016/j.biopha.2019.108746
42. Zhu B, Xue F, Li G, Zhang C. CRYAB promotes osteogenic differentiation of human bone marrow stem cells via stabilizing beta-catenin and promoting the Wnt signalling. *Cell Prolif*. 2020;53(1):e12709. doi:10.1111/cpr.12709
43. Sun L, Li Z, Xue H, et al. MiR-26a promotes fracture healing of nonunion rats possibly by targeting SOSTDC1 and further activating Wnt/beta-catenin signaling pathway. *Mol Cell Biochem*. 2019;460(1–2):165–173. doi:10.1007/s11010-019-03578-9
44. Nusse R, Varmus H. Three decades of Wnts: a personal perspective on how a scientific field developed. *EMBO J*. 2012;31(12):2670–2684. doi:10.1038/emboj.2012.146
45. Willert K, Nusse R. Wnt proteins. *Cold Spring Harb Perspect Biol*. 2012;4(9):a007864. doi:10.1101/cshperspect.a007864
46. Leucht P, Jiang J, Cheng D, et al. Wnt3a reestablishes osteogenic capacity to bone grafts from aged animals. *J Bone Joint Surg Am*. 2013;95 (14):1278–1288. doi:10.2106/JBJS.L.01502
47. Nemoto E, Sakisaka Y, Tsuchiya M, et al. Wnt3a signaling induces murine dental follicle cells to differentiate into cementoblastic/osteoblastic cells via an osterix-dependent pathway. *J Periodontal Res*. 2016;51(2):164–174. doi:10.1111/jre.12294
48. Peng S, Gao D, Gao C, Wei P, Niu M, Shuai C. MicroRNAs regulate signaling pathways in osteogenic differentiation of mesenchymal stem cells (Review). *Mol Med Rep*. 2016;14(1):623–629. doi:10.3892/mmr.2016.5335
49. Long H, Sun B, Cheng L, et al. miR-139-5p represses BMSC osteogenesis via targeting Wnt/beta-catenin signaling pathway. *DNA Cell Biol*. 2017;36(8):715–724. doi:10.1089/dna.2017.3657
50. Duan L, Zhao H, Xiong Y, et al. MiR-16-2* interferes with WNT5A to regulate osteogenesis of mesenchymal stem cells. *Cell Physiol Biochem*. 2018;51(3):1087–1102. doi:10.1159/000495489
51. Ai G, Meng M, Wang L, et al. microRNA-196a promotes osteogenic differentiation and inhibit adipogenic differentiation of adipose stem cells via regulating beta-catenin pathway. *Am J Transl Res*. 2019;11(5):3081–3091.
52. Li B, Wang S, Wang S. MiR-195 suppresses colon cancer proliferation and metastasis by targeting Wnt3a. *Mol Genet Genomics*. 2018;293 (5):1245–1253. doi:10.1007/s00438-018-1457-y
53. Yang Y, Li M, Chang S, et al. MicroRNA-195 acts as a tumor suppressor by directly targeting Wnt3a in HepG2 hepatocellular carcinoma cells. *Mol Med Rep*. 2014;10(5):2643–2648. doi:10.3892/mmr.2014.2526
54. Chang M, Lin H, Fu H, Wang B, Han G, Fan M. MicroRNA-195-5p regulates osteogenic differentiation of periodontal ligament cells under mechanical loading. *J Cell Physiol*. 2017;232(12):3762–3774. doi:10.1002/jcp.25856
55. Gullotta F, Di Masi A, Ascenzi P. Carbon monoxide: an unusual drug. *IUBMB Life*. 2012;64(5):378–386. doi:10.1002/iub.1015

56. Mitchell LA, Channell MM, Royer CM, Ryter SW, Choi AMK, McDonald JD. Evaluation of inhaled carbon monoxide as an anti-inflammatory therapy in a non human primate model of lung inflammation. *Am J Physiol Lung Cell Mol Physiol*. 2010;299(6):L891–L897. doi:10.1152/ajplung.00366.2009
57. Bathoorn E, Slebos D, Postma DS, et al. Anti-inflammatory effects of inhaled carbon monoxide in patients with COPD: a pilot study. *Eur Respir J*. 2007;30(6):1131–1137. doi:10.1183/09031936.00163206
58. Mishra S, Fujita T, Lama VN, et al. Carbon monoxide rescues ischemic lungs by interrupting MAPK-driven expression of early growth response 1 gene and its downstream target genes. *Proc Natl Acad Sci USA*. 2006;103(13):5191–5196. doi:10.1073/pnas.0600241103
59. Tsui TY, Obed A, Siu YT, et al. Carbon monoxide inhalation rescues mice from fulminant hepatitis through improving hepatic energy metabolism. *Shock*. 2007;27(2):165–171. doi:10.1097/01.shk.0000239781.71516.61
60. Foresti R, Bani-Hani MG, Motterlini R. Use of carbon monoxide as a therapeutic agent: promises and challenges. *Intensive Care Med*. 2008;34(4):649–658. doi:10.1007/s00134-008-1011-1
61. Foresti R, Bani-Hani MG, Motterlini R. Use of carbon monoxide as a therapeutic agent: promises and challenges. *Intensive Care Med*. 2008;34(4):649–658. doi:10.1007/s00134-008-1011-1
62. Adach W, Olas B. Carbon monoxide and its donors – their implications for medicine. *Future Med Chem*. 2019;11(1):61–73. doi:10.4155/fmc-2018-0215
63. Ji X, Damera K, Zheng Y, Yu B, Otterbein LE, Wang B. Toward carbon monoxide-based therapeutics: critical drug delivery and developability issues. *J Pharm Sci*. 2016;105(2):406–416. doi:10.1016/j.xphs.2015.10.018